



PERGAMON

International Journal of Solids and Structures 40 (2003) 4943–4954

INTERNATIONAL JOURNAL OF
SOLIDS and
STRUCTURES

www.elsevier.com/locate/ijsolstr

Simulation of impact between rigid elements

Gabriel Barrientos ^{a,*}, Luis Baeza ^b

^a Department of Mechanical Engineering, University of Concepción, Casilla 160-C, Concepción, Chile

^b Industrial Support Ltda., Suecia 84. Of.43, Providencia, Santiago, Chile

Received 28 August 2002; received in revised form 30 December 2002

Abstract

The objective of this paper is to apply the concepts and theories of global impact based on a modern formulation in which the impact is considered with sliding, adherence or transition between sliding and adherence. The energy dissipated in the contact may be quantified by different definitions of the coefficient of restitution in Newton's law and Poisson's law. The method is applied to the impact between the damper (parabolic elements) and the platform of the blades in an airborne gas turbine. A numerical solution is calculated using a computer program constructed on the Matlab Platform.

© 2003 Elsevier Ltd. All rights reserved.

Keywords: Impact; Non-linear mechanics; Restitution coefficient; Friction; Sliding

1. Introduction

Impact occurs when two bodies collide. This event is usually very short (Brach, 1984; Keller, 1986; Smith and Liu, 1992). Deformations occur in both bodies, caused first by a compression phase, then by an expansion phase. Forces generated depend upon the kinematics, initial conditions and contact dynamics. Impact ends when the normal force between the two bodies tends to zero. Generally, impact is accompanied by sliding, adherence or transition between sliding and adherence, due to the relative tangential velocity between the contact surfaces. Contact between bodies is generally dissipative. Energy dissipated in the contact may be quantified by the coefficients in Newton's law, Poisson's law, and Stronge's law (Stronge, 1990). Different definitions of the coefficient of restitution give different results depending on the values of friction, direction of approach velocities, and inertia characteristics of the system.

*Corresponding author. Fax: +56-41-251142.

E-mail addresses: gbarrien@udec.cl (G. Barrientos), lbaeza@highservice.cl (L. Baeza).

2. Distance between bodies

Fig. 1 shows how the distance between two bodies is defined. Each body may have a rotational velocity Ω and a rotational acceleration $\dot{\Omega}$. The body-fixed point P may move by a velocity v_P and may be accelerated by a_P . The smooth and planar contour Σ of the body is assumed to be convex and can be described in parametric form by the vector ${}_B r_{P\Sigma}$, using the body-fixed frame B. The parameter s corresponds to the arc length of the body. Thus, the moving trihedral ($\mathbf{t}, \mathbf{n}, \mathbf{b}$) in the curve can be stated in frame B: ${}_B \mathbf{n} = {}_B \mathbf{b} \times {}_B \mathbf{t}$, with κ as the curvature of the contour at point P: $\kappa_B \mathbf{n} = {}_B \mathbf{b}''_{P\Sigma}$, where $('') = d^2() / ds^2$. The normal \mathbf{n} always points inward and is directed to the center of the circle of curvature.

The sense of rotation of the curve parameters s_1, s_2 is chosen so that the binormals of both moving trihedrals are the same, $\mathbf{b}_1 = \mathbf{b}_2$. The origins of the trihedrals are connected by a distance vector \mathbf{r}_D . In order to derive the distance between the bodies it is necessary to satisfy the non-linear problem:

$$\mathbf{n}_1^T(s_1) \cdot \mathbf{t}_2(s_2) = 0 \iff \mathbf{n}_2^T(s_2) \cdot \mathbf{t}_1(s_1) = 0 \quad (1)$$

$$\mathbf{r}_D^T(s_1, s_2) \cdot \mathbf{t}_1(s_1) = 0; \quad \mathbf{r}_D^T(s_1, s_2) \cdot \mathbf{t}_2(s_2) = 0 \quad (2)$$

It is necessary that one of Eqs. (1) and one of (2) are satisfied. The values (s_1, s_2) are called the “contact parameters”, and the corresponding points (C_1, C_2) the “contact points”. For this configuration the relations between the axes of both trihedrals are given by:

$$\mathbf{n}_1 = -\mathbf{n}_2; \quad \mathbf{t}_1 = -\mathbf{t}_2; \quad \mathbf{b}_1 = \mathbf{b}_2 \quad (3)$$

and the distance g_N between the bodies is determined by:

$$g_N(\mathbf{q}, t) = \mathbf{r}_D^T \mathbf{n}_2 = -\mathbf{r}_D^T \mathbf{n}_1 \quad (4)$$

3. Movement equations

A generalized coordinate system \mathbf{q} is chosen, so that velocity, acceleration or variation may be expressed in a linear form by means of the terms corresponding to the generalized coordinates. The equation of motion in a reduced form function of the generalized coordinates was presented by (Pfeiffer and Glocker, 1996):

$$\mathbf{M}(\mathbf{q}, t) \ddot{\mathbf{q}} - \mathbf{h}(\mathbf{q}, \dot{\mathbf{q}}, t) = \mathbf{0} \in \mathfrak{R}^f \quad (5)$$

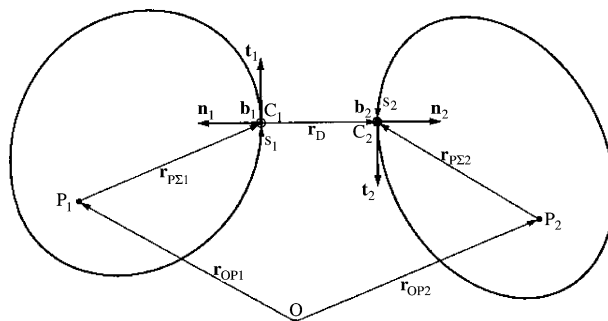


Fig. 1. Distance between bodies. General orientation trihedrals.

where f represents the degree of freedom, $\mathbf{M} \in \mathfrak{R}^{f \times f}$ is the matrix of mass, and $\mathbf{h} \in \mathfrak{R}^f$ is the vector which is the addition of all the movements and active forces. The contact forces in Eq. (5) are considered by using a Lagrangian approach, consisting of multiplying the forces of every body by the vectors of transformation that correspond, then adding them to Eq. (5). N and H represent the normal and tangential directions, respectively.

Now, if there is a system with n_G contact points, four groups of indices which describe the kinematic state of every contact are introduced.

$$\begin{aligned} I_G &= \{1, 2, \dots, n_G\} \\ I_S &= \{i \in I_G | g_{N_i} = 0\} \quad \text{with } n_S \text{ elements} \\ I_N &= \{i \in I_S | \dot{\mathbf{g}}_{N_i} = 0\} \quad \text{with } n_N \text{ elements} \\ I_H &= \{i \in I_N | \dot{\mathbf{g}}_{H_i} = 0\} \quad \text{with } n_H \text{ elements} \end{aligned} \quad (6)$$

The I_G group corresponds to the n_G number of all the contact points, I_S consists of the n_S indices with relative distance zero, but with an arbitrary relative velocity, I_N represents the restrictions that are necessary for a continuous contact (null distance and zero relative velocity in the normal direction), and I_H are the adherence points. Dividing tangential forces into the sliding and adherence forces and writing the equations as a matrix:

$$\begin{aligned} \mathbf{M}\ddot{\mathbf{q}} - \mathbf{h} - [\mathbf{W}_N + \mathbf{W}_G \boldsymbol{\mu}_G \quad \mathbf{W}_H] \begin{pmatrix} \boldsymbol{\lambda}_N \\ \boldsymbol{\lambda}_H \end{pmatrix} &= \mathbf{0} \in \mathfrak{R}^f \\ \begin{pmatrix} \ddot{\mathbf{g}}_N \\ \ddot{\mathbf{g}}_H \end{pmatrix} &= \begin{pmatrix} \mathbf{W}_N^T \\ \mathbf{W}_H^T \end{pmatrix} \ddot{\mathbf{q}} + \begin{pmatrix} \boldsymbol{\omega}_N \\ \boldsymbol{\omega}_H \end{pmatrix} \in \mathfrak{R}^{n_N + n_H} \end{aligned} \quad (7)$$

Here, $\boldsymbol{\mu}_G$ is a matrix diagonal that contains all the coefficients of friction of the points of sliding, \mathbf{W}_N , \mathbf{W}_G , \mathbf{W}_H are matrices of transformation between the generalized coordinates and the local coordinates, $(\boldsymbol{\lambda}_N \quad \boldsymbol{\lambda}_H)^T$ vector normal and tangential force, and $(\boldsymbol{\omega}_N \quad \boldsymbol{\omega}_H)^T$ are acceleration vectors that relate the generalized coordinates with the local coordinates.

Newton's law is one of the most used laws in case of impact, and it connects the normal relative velocity before and after the impact: $\dot{\mathbf{g}}_{NE} = -\bar{\epsilon}_N \dot{\mathbf{g}}_{NA} \cdot \bar{\epsilon}_N = \text{diag}\{\epsilon_{N_i}\}$, which contains the n_S^* coefficients of restitution whose values range between $0 \leq \epsilon_{N_i} \leq 1$. Replacing Newton's law, the velocity in generalized coordinates after the impact is $\dot{\mathbf{q}}_E = \dot{\mathbf{q}}_A - \mathbf{M}^{-1} \mathbf{W}_N \mathbf{G}_N^{-1} (\mathbf{I} + \bar{\epsilon}) \dot{\mathbf{g}}_{NA}$. Here, \mathbf{I} is a matrix identity, and \mathbf{G}_N is the effective mass matrix. Another option is Poisson's law, which connects the normal impulse of expansion with the impulse of compression ($\Lambda_{NE} = -\bar{\epsilon} \Lambda_{NC}$), where $\Lambda_{NC} = \lim_{t_C \rightarrow 0} \int_{t_A}^{t_C} \lambda_{N_i} dt_i$ represent the normal impulse of compression, and Λ_{HC} the tangential impulse. This law is generally applied to systems with friction, so it can be attached with Coulomb's law.

4. Example (Baeza, 2000)

This theory is applied to a problem of contact between a parabolic element of friction, which occurs between the platform and the blades in an aeroplane's gas turbine. It can be modeled as a problem of contact between a parabola (damper) and a right line (blades' base), shown in Fig. 2.

The quadruple coordinates $\mathbf{q} = (z, \varphi, x, y)^T$ must be used to describe the displacements of the platform and the damper, where z describes the horizontal position of the base fixed to the platform, and (φ, x, y) describe the displacements and rotation of the damper. The outlines under investigation are Σ_1 and Σ_2 .

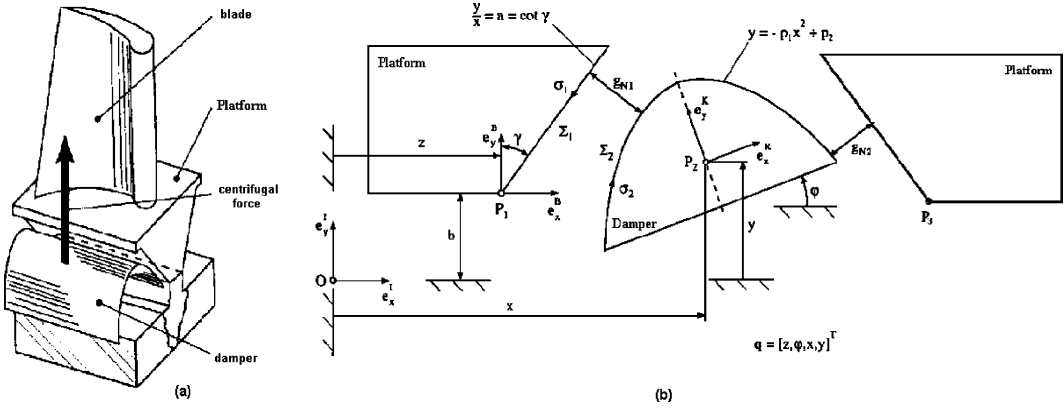


Fig. 2. Problem of contact in a turbine: (a) Turbine physical representation and (b) mechanical model.

They are described by the functions $y = ax$ and $y = -p_1x^2 + p_2$, in relation to the coordinates B and K fixed to the bodies. The movement equation of the parabola is given by:

$$\begin{pmatrix} m & 0 & 0 \\ 0 & m & 0 \\ 0 & 0 & I_p \end{pmatrix} \begin{pmatrix} \ddot{x} \\ \ddot{y} \\ \ddot{\varphi} \end{pmatrix} + \begin{pmatrix} 0 \\ mg \\ 0 \end{pmatrix} = \begin{pmatrix} 0 \\ 0 \\ 0 \end{pmatrix} \quad (8)$$

where g is the gravity acceleration, m is a mass, and I_p the inertia of parabola. The distance in the normal direction is given by:

$$g_N = \frac{1}{\sqrt{1+a^2}} [b - y + ax - az - (p_1\sigma_2^2 + p_2)(a \sin \varphi + \cos \varphi)] \quad (9)$$

where the normal relative velocity (N) and tangential relative velocity (H) are:

$$\dot{\mathbf{g}}_N = \boldsymbol{\omega}_N^T \dot{\mathbf{q}} + \boldsymbol{\omega}_N; \quad \dot{\mathbf{g}}_H = \boldsymbol{\omega}_H^T \dot{\mathbf{q}} + \boldsymbol{\omega}_H \quad (10)$$

with

$$\boldsymbol{\omega}_N^Y = \frac{1}{\sqrt{1+a^2}} \left[-a \quad \left(\frac{1}{2p_1} + p_1\sigma_2^2 - p_2 \right) (a \cos \varphi - \sin \varphi) \quad a \quad -1 \right]; \quad \boldsymbol{\omega}_N = 0$$

$$\boldsymbol{\omega}_H^Y = \frac{1}{\sqrt{1+a^2}} \left[-1 \quad -(p_1\sigma_2^2 - p_2)(a \sin \varphi - \cos \varphi) \quad 1 \quad a \right]; \quad \boldsymbol{\omega}_H = 0$$

A computational program that resolves the movement equations using the fourth-order method of Runge–Kutta in MATLAB is implemented. It is supposed that both platforms have infinite mass, and point P_2 coincides with the center of gravity of the parabolic damper (Table 1).

Analysis of the impact is first divided in two phases: compression and expansion, obtaining the following equations:

Phase of compression (C):

$$\begin{pmatrix} \dot{\mathbf{g}}_{NC} \\ \dot{\mathbf{g}}_{HC} \end{pmatrix} = \begin{pmatrix} \mathbf{W}_N^T \\ \mathbf{W}_H^T \end{pmatrix} \dot{\mathbf{q}}_C + \begin{pmatrix} \boldsymbol{\omega}_N \\ \boldsymbol{\omega}_H \end{pmatrix} \quad (11)$$

Table 1

General data for contact between the platform of the blade and the damper in airborne gas turbine

| Data | x | y | φ |
|---|-----|---------------------|-----------|
| Position of point P ₁ | 1 m | 3 m | 0 |
| Position of point P ₃ | 8 m | 9 m | 0 |
| Velocity and acceleration | 0 | 0 | 0 |
| Tangent of the straight line | | 2.5 | |
| Position of point P ₂ | 5 | 8 | 0 |
| Velocity of point P ₂ | -4 | 12 | 0 |
| Parabola parameters | | $p_1 = -2; p_2 = 2$ | |
| Parabola mass: m (kg) | | 10 | |
| Inertia of parabola: I (kg m ²) | | 30 | |

$$\mathbf{M}(\dot{\mathbf{q}}_C - \dot{\mathbf{q}}_A) - (\mathbf{W}_N \quad \mathbf{W}_H) \begin{pmatrix} \Lambda_{NC} \\ \Lambda_{HC} \end{pmatrix} = \mathbf{0} \quad (12)$$

and the complementary condition:

$$\Lambda_{NC} \cdot \dot{\mathbf{g}}_{NC} = 0; \quad \Lambda_{NC} \geq 0; \quad \dot{\mathbf{g}}_{NC} \geq 0 \quad (13)$$

Phase of expansion (E):

$$\begin{pmatrix} \dot{\mathbf{g}}_{NE} \\ \dot{\mathbf{g}}_{HE} \end{pmatrix} = \begin{pmatrix} \mathbf{W}_N^T \\ \mathbf{W}_H^T \end{pmatrix} \dot{\mathbf{q}}_E + \begin{pmatrix} \boldsymbol{\omega}_N \\ \boldsymbol{\omega}_H \end{pmatrix} \quad (14)$$

$$\mathbf{M}(\dot{\mathbf{q}}_E - \dot{\mathbf{q}}_C) - (\mathbf{W}_N \quad \mathbf{W}_H) \begin{pmatrix} \Lambda_{NE} \\ \Lambda_{HE} \end{pmatrix} = \mathbf{0} \quad (15)$$

and the complementary condition:

$$\Lambda_{NE} \dot{\mathbf{g}}_{NE} = 0; \quad \Lambda_{NE} \geq 0; \quad \dot{\mathbf{g}}_{NE} \geq 0 \quad (16)$$

The friction term relates the distance and tangential velocity between the bodies if there is sliding and adhesion. Clearing the normal and tangential velocity in each phase, it is obtained as:

Compression

$$\begin{cases} \dot{\mathbf{g}}_{NC} = A\Lambda_{NC} + B\Lambda_{TC} + \dot{\mathbf{g}}_{NA} \\ \dot{\mathbf{g}}_{HC} = B\Lambda_{NC} + C\Lambda_{HC} + \dot{\mathbf{g}}_{HA} \end{cases} \quad (17)$$

expansion

$$\begin{cases} \dot{\mathbf{g}}_{NE} = A\Lambda_{NE} + B\Lambda_{TE} + \dot{\mathbf{g}}_{NC} \\ \dot{\mathbf{g}}_{HE} = B\Lambda_{NE} + C\Lambda_{HE} + \dot{\mathbf{g}}_{HC} \end{cases} \quad (18)$$

with

$$A = \boldsymbol{\omega}_N^T \mathbf{M}^{-1} \boldsymbol{\omega}_N; \quad B = \boldsymbol{\omega}_N^T \mathbf{M}^{-1} \boldsymbol{\omega}_H; \quad C = \boldsymbol{\omega}_H^T \mathbf{M}^{-1} \boldsymbol{\omega}_H \quad (19)$$

$\dot{\mathbf{g}}_{NC} = \mathbf{0}$ is the velocity at the end of the compression phase. The simulations are made supposing that the damper moves and the platform stay fixed. With the equations of the raised movement and theories of shock, a computational program is implemented that shows the occurrence of the shock and

gives results of positions, velocities, accelerations, energies, and forces of impact. The following cases are studied.

4.1. Newton's law without friction

In this case, the tangential component has no influence ($\dot{\mathbf{g}}_{HA} = \dot{\mathbf{g}}_{HE}$) since velocity is maintained in that direction and the results depend exclusively on the normal components and the coefficient of restitution. Using the law of Newton ($\dot{\mathbf{g}}_{NE} = -\epsilon \dot{\mathbf{g}}_{NA}$), the normal impulse is given by: $\Lambda_{NC} = -(\dot{\mathbf{g}}_{NA}/A)$, with $A = \omega_N^T \mathbf{M}^{-1} \omega_N$. Using the law of Poisson, $\Lambda_{NE} = \epsilon \Lambda_{NA}$, the normal impulse of compression is given by $\Lambda_{NC} = -(\dot{\mathbf{g}}_{NA}/A)$. The normal velocity at the end of the expansion is given by $\dot{\mathbf{g}}_{NE} = A \Lambda_{NE}$. When the impulse is replaced: $\dot{\mathbf{g}}_{NE} = -(A \epsilon \dot{\mathbf{g}}_{NA}/A) = -\epsilon \dot{\mathbf{g}}_{NA}$. Therefore, when friction is not considered, the theories are analogous. The results for $\epsilon = 1$ appear in Fig. 3. In this case they are the results indicated in Table 2. Fig. 3a and b show an animation of the movement and shocks of the bodies. Fig. 3c indicates how the normal distance \mathbf{g}_N varies between the bodies that collide, and Fig. 3d shows the variation of the energy. The total energy of the system stays constant (impact completely elastic).

4.2. Contact problems with friction

If friction is considered, we can analyze some situations of interest depending upon the theory of impact used.

4.2.1. Newton's law with adherence

For the bodies to adhere, during the compression phase $\dot{\mathbf{g}}_{HC} = \mathbf{0}$, and thus, using (17):

$$\Lambda_{NC} = \frac{(B\dot{\mathbf{g}}_{HA} - C\dot{\mathbf{g}}_{NA})}{(CA - B^2)} y; \text{ and } \Lambda_{HC} = \frac{-(A\Lambda_{NC} + \dot{\mathbf{g}}_{NC})}{B}$$

For the expansion phase, normal velocity is given by $\dot{\mathbf{g}}_{NE} = -\epsilon \dot{\mathbf{g}}_{NA}$, and the tangential velocity due to the adhesion is zero ($\dot{\mathbf{g}}_{HE} = \mathbf{0}$). The results are shown in Fig. 4 and Table 3 shows some values obtained. Impact with adherence produces rotation in a parabola. Fig. 4a shows the central point movement and Fig. 4c shows the large loss of energy in the first impact.

4.2.2. Newton's law with sliding

When sliding occurs, Coulomb's law applies. The phase of compression is $\Lambda_{HC} = \pm \mu \Lambda_{NC}$, where the sense of the tangential impulse must be inverse to $\dot{\mathbf{g}}_{HA}$. Replacing $\dot{\mathbf{g}}_{HA}$ in Eq. (17):

$$\Lambda_{NC} = \frac{-\dot{\mathbf{g}}_{NA}}{(A - \mu B)}$$

The tangential velocity at the end of the compression phase is $\dot{\mathbf{g}}_{HC} = A\Lambda_{NC} + B\Lambda_{HC} + \dot{\mathbf{g}}_{HA}$. For the expansion phase, by the law of Newton: $\dot{\mathbf{g}}_{NE} = -\epsilon \dot{\mathbf{g}}_{NA}$. In addition, by the law of Coulomb: $\Lambda_{HE} = \mu \Lambda_{NE}$. Replacing these quantities in Eq. (18):

$$\Lambda_{NE} = \frac{\epsilon \dot{\mathbf{g}}_{NE}}{(A - \mu B)}$$

where the tangential velocity at the end of the impact is $\dot{\mathbf{g}}_{HE} = B\Lambda_{NE} + C\Lambda_{HE} + \dot{\mathbf{g}}_{HC}$. The results obtained are shown in Fig. 5 and Table 4, for the case of $\mu = 0.5$.

4.2.3. Poisson law with adherence

Adhesion requires that $\dot{\mathbf{g}}_{HC} = \mathbf{0}$. Replacing this value in the compression phase of (17) yields:

$$\Lambda_{NC} = \frac{(B\dot{\mathbf{g}}_{HA} - C\dot{\mathbf{g}}_{NA})}{(CA - B^2)} \quad \text{and} \quad \Lambda_{HC} = \frac{-(A\dot{\mathbf{g}}_{NC} + \dot{\mathbf{g}}_{NC})}{B}$$

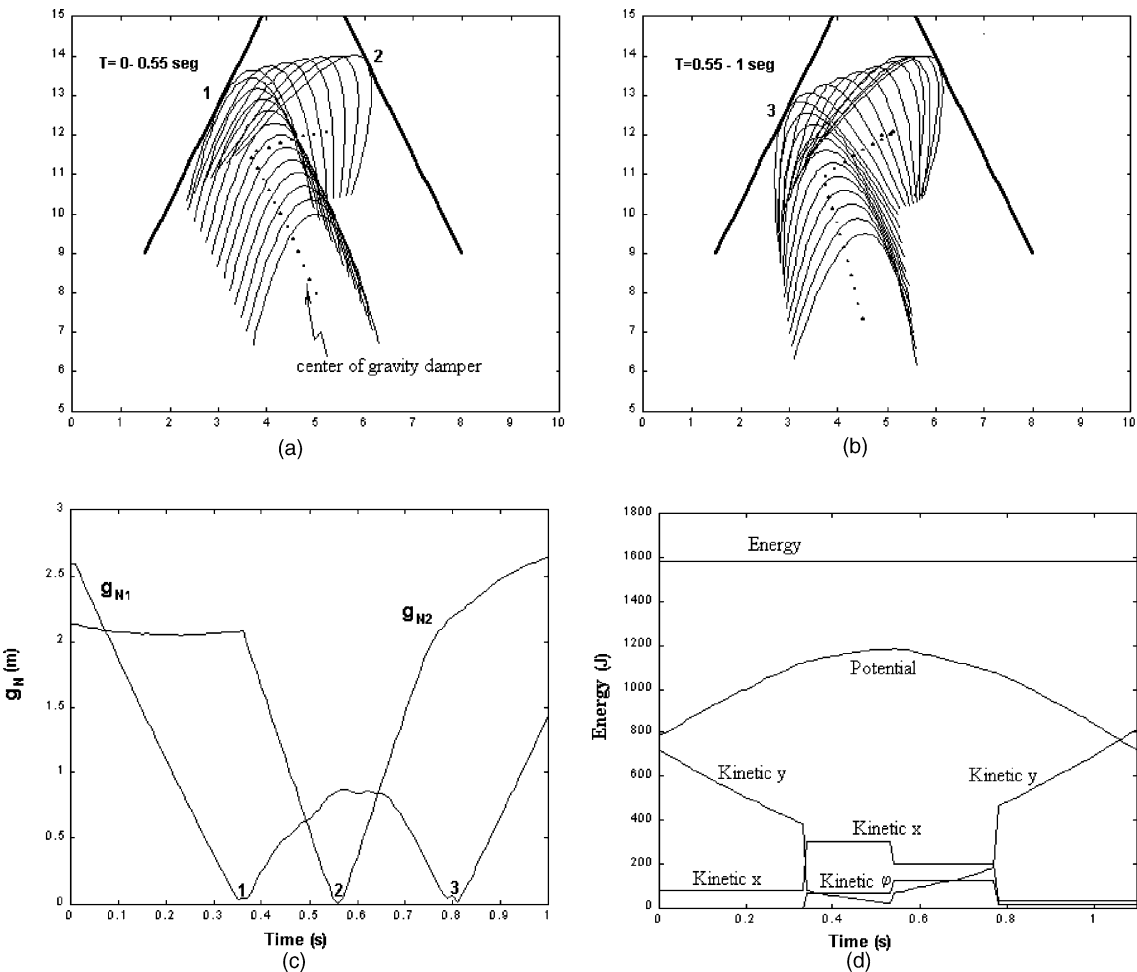


Fig. 3. (a), (b) Animation by Newton without friction, (c) variation of normal distance and (d) energy variations.

Table 2
Impact time and velocities in Newton's law without friction (Fig. 3)

| Impacts | Point 1 | Point 2 | Point 3 |
|----------------------|---------|---------|---------|
| Time (s) | 0.34 | 0.54 | 0.78 |
| \dot{g}_{NA} (m/s) | -6.93 | -10.18 | -7.24 |
| \dot{g}_{TA} (m/s) | 6.56 | 4.72 | -11.84 |
| Λ_{NC} (N s) | 63.79 | 76.52 | 48.01 |

For the expansion phase, Poisson's law requires that $\Lambda_{NE} = \epsilon \Lambda_{NC}$, which when replaced in (18) yields:

$$\Lambda_{HE} = \frac{-B\Lambda_{NE}}{C} \quad (20)$$

where the normal speed at the end of the expansion is $\dot{g}_{NE} = A\Lambda_{NE} + B\Lambda_{HE}$. The results are shown in Fig. 6 and Table 5.

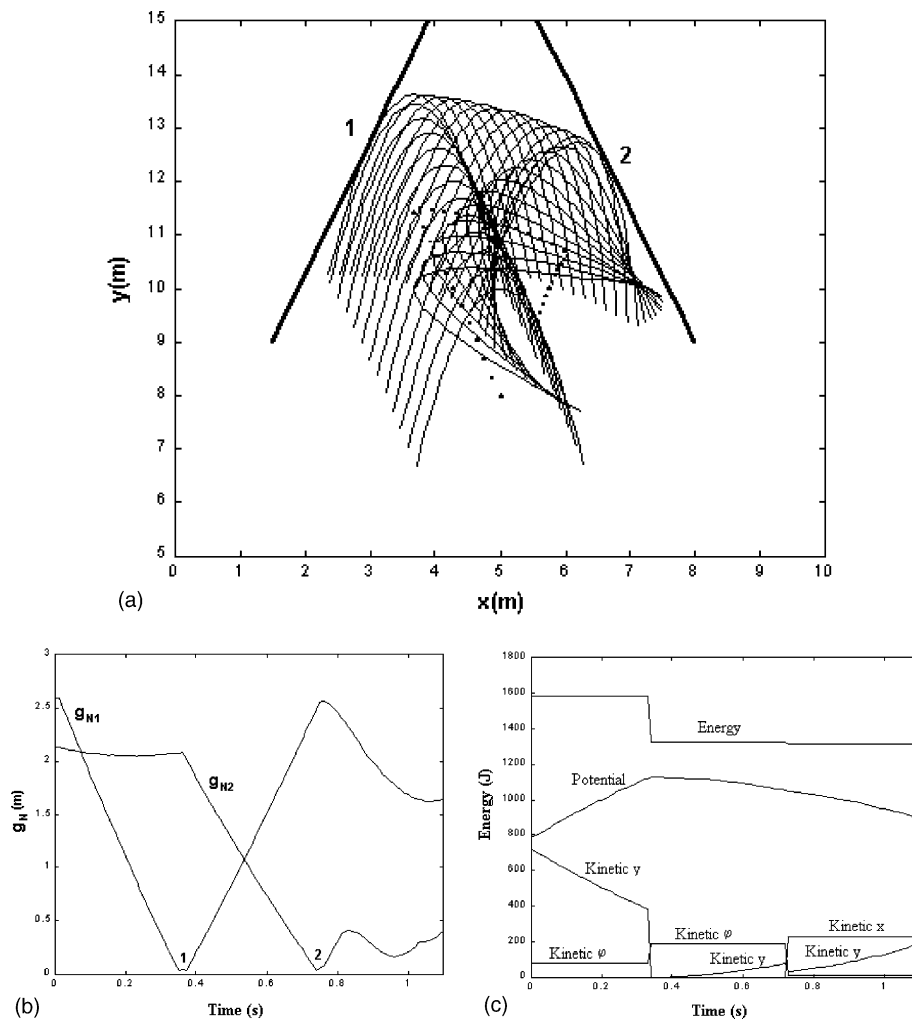


Fig. 4. (a) Animation by Newton with adherence, (b) variations of normal distance and (c) energy variations.

Table 3
Impact time and velocities in Newton's law with adherence (Fig. 4)

| Impacts | Point 1 | Point 2 |
|----------------------|---------|---------|
| Time (s) | 0.34 | 0.73 |
| \dot{g}_{NA} (m/s) | -6.93 | -4.71 |
| \dot{g}_{HA} (m/s) | 6.56 | 6.54 |
| Λ_{NC} | 73.98 | 20.53 |
| Λ_{HC} | -54.79 | -36.94 |

The figures show that three impacts occur. Table 5 shows that the tangential impulse has the opposite sense to the tangential velocity. The greatest loss of energy occurs in the third impact, and is a product of the greater tangential velocity.

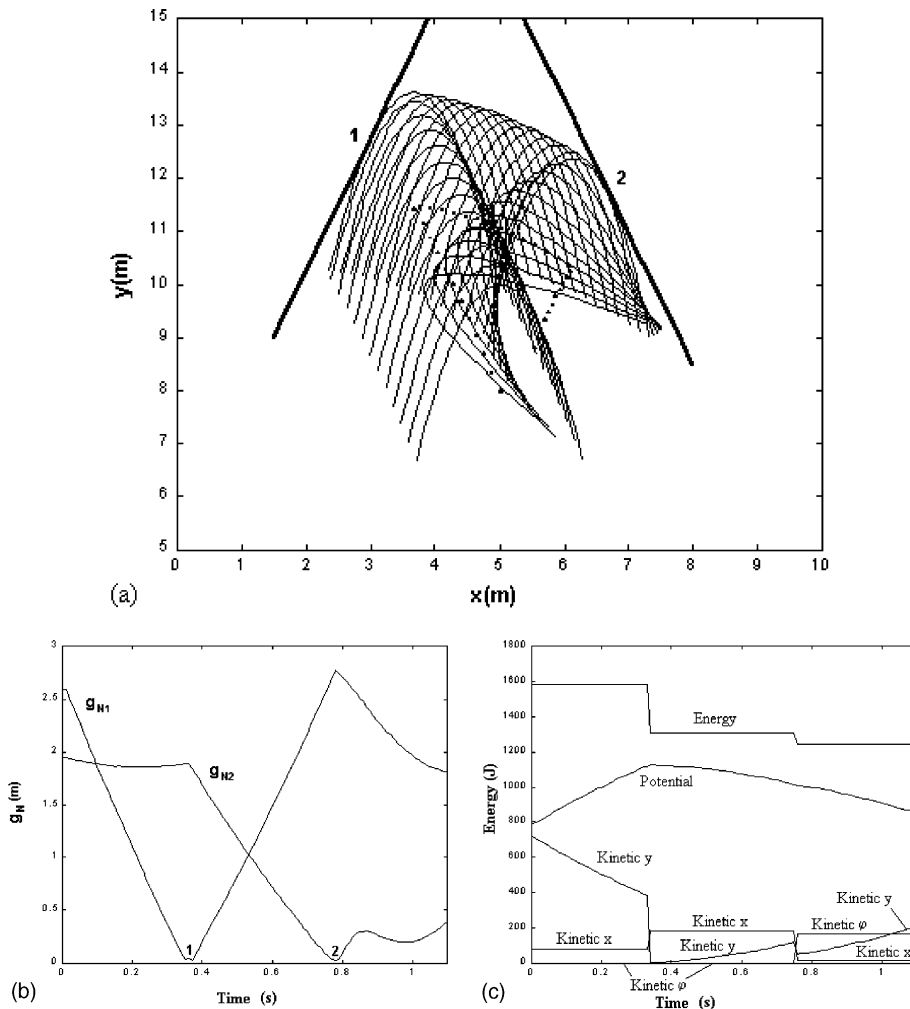


Fig. 5. (a) Animation by Newton with sliding, (b) variations of normal distance and (c) energy variations.

Table 4
Impact time and velocities in Newton's law with adherence (Fig. 5)

| Impacts | Point 1 | Point 2 |
|----------------------|---------|---------|
| Time (s) | 0.34 | 0.76 |
| \dot{g}_{NA} (m/s) | -6.93 | -3.80 |
| \dot{g}_{TA} (m/s) | 6.56 | 6.97 |
| Λ_{NC} (N s) | 70.33 | 29.37 |
| Λ_{TC} (N s) | -35.17 | -14.69 |

4.2.4. Poisson law with sliding

First, the law of Coulomb is considered, which in the compression phase is $\Lambda_{HC} = \pm \mu \Lambda_{NC}$, where the sense of the tangential impulse must be inverse to \dot{g}_{HA} . Replacing these values in Eq. (18) yields

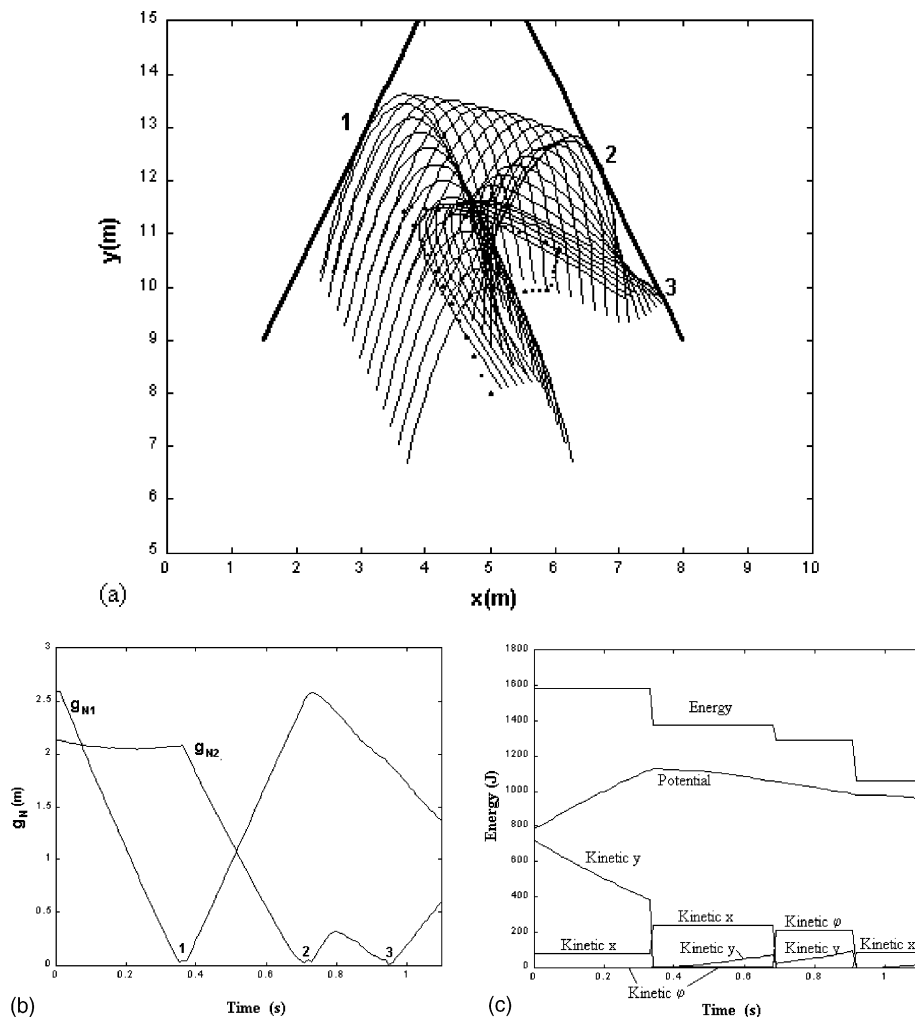


Fig. 6. (a) Animation by Poisson with adherence, (b) variations of normal distance and (c) energy variations.

Table 5
Impact time and velocities in Newton's law with adherence (Fig. 6)

| Impacts | Point 1 | Point 2 | Point 3 |
|-----------------------------|---------|---------|---------|
| Time (s) | 0.34 | 0.69 | 0.92 |
| \dot{g}_{NA} (m/s) | -6.93 | -5.61 | -3.52 |
| \dot{g}_{TA} (m/s) | 6.56 | 6.96 | 9.77 |
| Λ_{NC} (Ns) | 73.98 | 26.98 | 5.09 |
| Λ_{TC} (Ns) | -54.79 | -36.04 | -56.25 |

$$\Lambda_{\text{NC}} = \frac{-\dot{g}_{\text{NA}}}{(A - \mu B)} \quad (21)$$

The tangential velocity at the end of the compression phase is given by $\dot{g}_{\text{HC}} = A\Lambda_{\text{NC}} + B\Lambda_{\text{HC}} + \dot{g}_{\text{HA}}$. For the phase of expansion $\Lambda_{\text{NE}} = \epsilon\Lambda_{\text{NA}}$, and from Coulomb's law, $\Lambda_{\text{HE}} = \mu\Lambda_{\text{NE}}$. Replacing these values in (18)

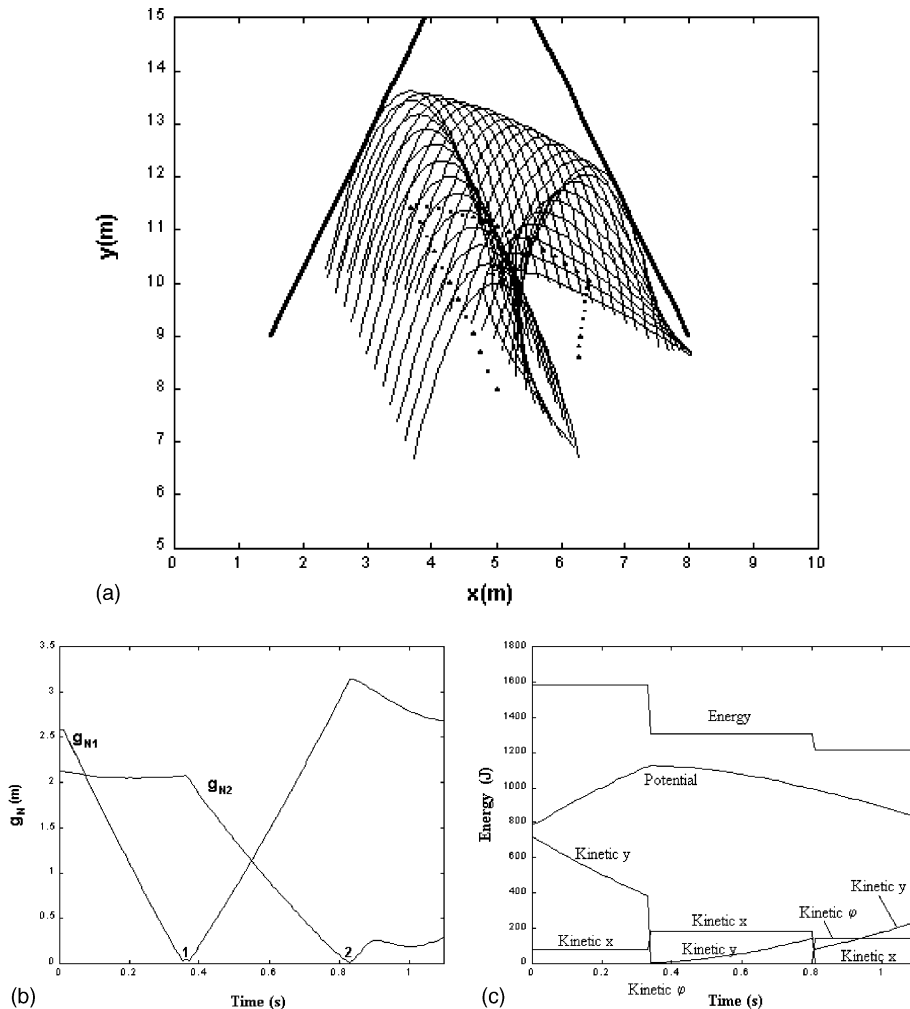


Fig. 7. (a) Animation by Poisson with sliding, (b) variations of normal distance and (c) energy variations.

Table 6
Impact time and velocities in Poisson's law with sliding (Fig. 7)

| Impacts | Point 1 | Point 2 |
|-----------------------|---------|---------|
| Time (s) | 0.34 | 0.81 |
| g _{NA} (m/s) | -6.93 | -3.66 |
| g _{TA} (m/s) | 6.56 | 7.41 |
| Λ _{NC} (N s) | 70.33 | 24.42 |
| Λ _{TC} (N s) | -35.17 | -12.21 |

yields $\Lambda_{NE} = (\epsilon g_{NE}/(A - \mu B))$, where the tangential velocity at the end of the impact is $\dot{g}_{HE} = B\Lambda_{NE} + C\Lambda_{HE} + \dot{g}_{HC}$. The results are shown in Fig. 7 and Table 6 for the case of $\mu = 0.5$. Fig. 7 shows two impacts. Due to friction, energy is lost during each impact. The greater loss of energy takes place in the first impact, and is a product of the greater tangential velocity.

5. Conclusions

A program using MATLAB is available. It allows the solution of different configurations for impact between rigid bodies. The Runge-Kutta method was used to integrate equations of motion. The results of other examples (not shown in this paper) were compared with others obtained by different authors. They showed appropriate accuracy. An applied example is shown, where the choice of an adequate coefficient of restitution has great importance in determining what happens after the impact, as well as knowing what would happen in subsequent impacts. A comparison of the results obtained by using Newton's and Poisson's theories, shows that they are different in every case.

References

Baeza, L., 2000. Simulación de choque entre elementos rígidos. Memoria de Título Ingeniero Civil Mecánico. Universidad de Concepción, Chile.

Brach, R.M., 1984. Friction, restitution and energy loss in planar collisions. Transaction of ASME 51, 164–170.

Keller, J.B., 1986. Impact with friction. Journal of Applied Mechanics 53, 1–4.

Pfeiffer, F., Glocker, Ch., 1996. Multibody dynamics with unilateral contacts. Wiley Series in Nonlinear Science. John Wiley and Sons Inc., New York.

Smith, Ch., Liu, P.-P., 1992. Coefficients of restitution. Journal of Applied Mechanics 59, 963–969.

Stronge, W.J., 1990. Rigid body collisions with friction. Proceedings of the Royal Society of London A 431, 169–181.